Statistically accurate length measurements of single-walled carbon nanotubes

Kirk J. Ziegler, Zhenning Gu, Robert H. Hauge, and Richard E. Smalley [*]

Department of Chemistry, Center for Nanoscale Science and Technology, Rice University, Houston, Texas 77005, USA

[*] Corresponding author: Tel: 713-348-3250; Fax: 713-348-5320; email: res@rice.edu

Abstract

The ability to accurately measure the length of nanotubes is important to understanding nanotube growth and cutting processes. To date, there have been few methods available to obtain a statistically significant length measurement of any nanotube sample due to difficulties in obtaining a complete suspension of individuals and the tedious nature of measuring 1000+ nanotubes. Here we describe a relatively simple method that functionalizes single-walled carbon nanotubes to achieve a high propensity of individuals in chloroform as high as 92%. This suspension can be dispersed on mica substrates for AFM analysis. Nanotube lengths and heights can be determined using the Nanotube Length Analysis module of SIMAGIS yielding an accurate measure of length and height distribution of a large population of the nanotube sample.

Single-walled carbon nanotubes (SWNTs) offer unique electronic and mechanical properties [1, 2]. Therefore, many applications have been envisioned which utilize these properties, such as strong lightweight composites, electronics, and biological imaging or sensing. However, before SWNTs can be utilized for widespread applications, many issues need to be resolved. Growth mechanisms of SWNTs are not well understood including the ability to increase yield or control their chirality and length. Some

nanotube applications such as field-effect transistors [3] or biological imaging may require individual short nanotubes. To achieve these short lengths, SWNTs can be cut through a variety of processes [4-7]. A key step to understanding nanotube growth and cutting processes is the accurate measurement of the nanotube length.

While some progress has been made with in-situ techniques [8-10], these approaches typically only give an average length and no information about the distribution. Direct imaging techniques are more tedious but typically give more information. Of these imaging approaches, AFM appears to be the most useful technique [4, 11]. However, accurate measurements require two key steps: (i) suspension of the individual nanotubes in a solvent for dispersion onto a substrate and (ii) the length measurement of a statistically significant number of nanotubes. Many prior reports have utilized AFM as a means of measuring the length distribution but rarely have more than 100 nanotubes in their population. This stems from the difficulties in achieving the suspension of individual nanotubes and the tedious nature of measuring the length of 1000+ nanotubes. Here we describe a simple and efficient means of measuring a large population of nanotube lengths.

The first key step to length measurement analysis is the suspension of the nanotubes. A multitude of functionalization chemistries have been developed to solubilize single-walled nanotubes [12, 13]. Many of these approaches, however, involve significant processing and/or give few individual nanotubes and a large portion of small bundles. The use of surfactants followed by centrifugation [14, 15] yield a significant amount of individuals but does not give an accurate representation of the sample since the

solution is decanted from the solids. Extensive and intense sonication may also seriously distort lengths due to sonication induced cutting of nanotubes.

The recent development of Billups chemistry on nanotube sidewalls have significantly aided the dispersion of nanotubes [16, 17]. This approach is a relatively simple reaction that requires placing the nanotubes in liquid ammonia. The addition of the lithium is found to intercalate the nanotube ropes allowing the efficient reaction of the alkyl chains to the nanotube sidewall. Typically, the degree of functionalization achieved is approximately 1 chain per 20 – 30 C atoms [16]. After functionalization, complete suspension of the nanotubes is achieved. For length analysis, dilute solutions on the order of 0.1 mg/mL are used to obtain the correct surface coverage for image analysis. These suspensions can then be spin-coated onto freshly cleaved mica substrates after brief, mild sonication (~1 min) yielding a high quantity of individual nanotubes as seen in the AFM (Digital Instruments Nanoscope IIIA) image shown in Figure 1a. As can be seen in the images and discussed further below, most of the nanotubes exist as individuals.

The second critical step is the measurement of a large population of nanotubes to achieve statistically meaningful lengths. The lack of a method that yielded high quantities of individuals often precluded the analysis of a significant number of nanotubes. These low yields would have required numerous AFM images to be collected to obtain statistically significant length measurements. The high yield of the Billups reaction allows the measurement of 1000+ nanotubes by the collection of a handful of images. To eliminate the tedious nature of manually measuring 1000+ nanotubes, the lengths are measured using the Nanotube Length Analysis module of the SIMAGIS

(Smart Imaging Technologies, Houston, Texas) software package. This new software package has the capability of automatically analyzing multiple AFM images to obtain statistically accurate length and height (diameter) measurements of the nanotubes contained in the sample as well as particle and SWNT rope populations. In less than 1 minute, the software can analyze a single AFM image and extract the relevant length and height information for analysis.

As can be seen in Figure 1b, the program is capable of recognizing the nanotubes in the image and tracing their lengths. The program is also able to simultaneously obtain an average height along the length of the nanotube; therefore, the final image differentiates individual nanotubes (green) from nanotube ropes (black). Typically, nanotubes with heights smaller than 2 nm are considered to be individuals due to the presence of the dodecyl chains. The 2 nm height limit is stringent and likely excludes some individuals from larger diameter nanotubes but is necessary to eliminate ropes of small diameter nanotubes. Length and height (diameter) distributions for both the individual nanotubes and the nanotube ropes are then calculated for multiple AFM images as shown in Figure 2 and 3. Statistics for each image can be collected as well as an overall statistical picture of all images processed. This allows the ability to identify possible sampling problems which can lead to erroneous length analysis. Note that although the AFM image appears to have long nanotubes, the statistics suggest that there is a very broad distribution in lengths with a majority of the sample existing as nanotubes shorter than 300 nm. Combining the statistics for individual nanotubes and ropes (bundles) as seen in Figure 4 indicates that these bundles typically consist of less than five nanotubes. The shaded region indicates those nanotubes considered to be

individuals. The data shows that 92% of the nanotubes measured are individuals. Similar measurements on other samples indicate that dodecylation via the Billups reaction typically achieves 75 – 90% individuals. In addition, there is no length effect on nanotube de-bundling suggesting that the Li used in the Billups reaction is indeed capable of intercalating the graphene layers even for very long nanotubes allowing sufficient sidewall attack of the alkyl radicals. Finally, the program will also identify particles within the images as seen in Figure 5 (shown in red on Figure 1). For example, the data distinctly indicate the presence of a bimodal distribution. This allows the analysis of metal catalyst particles and fullerenes present in raw nanotube samples which may give insight into growth processes.

In order to achieve accurate measurements and minimize user input, quality AFM images are required. Poor image quality can have drastic effects on the quality of the nanotube traces. For example, images that have a 'grainy' background will often yield ghost nanotubes. Other common AFM image artefacts will also yield false nanotube traces. The resolution of the image will affect the smallest length of nanotubes that can be accurately measured. Therefore, all AFM images should be taken at the maximum resolution at a scan size capable of visualizing both the longest and shortest nanotubes in the sample. In addition, it is important to achieve the appropriate surface coverage. Figure 6 illustrates AFM images with varying degrees of surface coverage. Although the software package can distinguish overlapping nanotubes, too high of surface coverage can cause significant problems. After the program traces the nanotubes in the AFM image, the user has the option of manually editing the trace lines. However, if the surface coverage is chosen correctly, manual adjustments are insignificant as seen in Figure 6.

Although numerous adjustments were made to the image with moderate surface coverage (Fig. 6b and 6c), the errors encountered changed the final measured length by less than 10%. This is not true for higher surface coverage images (Fig. 6e and 6f) which can change by 30% or more. Interestingly, the distribution does not change significantly after the manual adjustments. However, the tail of the distribution has considerably more long nanotubes suggesting that it is more difficult to measure the longest nanotubes. These nanotubes will have considerable overlap leading to erroneous nanotube traces. Therefore, shorter nanotube samples typically give more accurate results with minimal need for manual adjustments. To keep the user input to a minimum, a moderate surface coverage is the optimal choice. It maximizes the ability of the software to differentiate between overlapping nanotubes while being able to get significant statistics with a bare minimum of AFM images and user intervention.

In conclusion, the functionalization of SWNTs with dodecyl chains via a Billups reaction yields as high as 92% of the sample as individual nanotubes in a chloroform suspension. These suspensions can be utilized for AFM image analysis. With moderate surface coverage and quality AFM images, the Nanotube Length Analysis module of SIMAGIS is capable of differentiating between individual nanotubes, nanotube ropes, and particles with minimum user intervention. Analysis of multiple AFM images (<10), therefore, allows the measurement of a significant population of the sample obtaining an accurate length and diameter measurement of the sample.

Acknowledgements

We gratefully acknowledge financial support from the National Science Foundation, the Office of Naval Research, the Robert A. Welch Foundation, the Center for Biological and Environmental Nanotechnology, and the Air Force Office of Scientific Research.

Figure Captions

Figure 1 (color). (a) AFM image of nanotubes functionalized with dodecyl chains using the Billups chemistry. Note the high concentration of individual nanotubes that are dispersed on the mica substrate. (b) Nanotubes measured using the Nanotube Length Analysis package of the SIMAGIS software. Individual nanotubes are designated by a green color while the nanotube ropes are shown in black. Particles are also shown in red.

Figure 2. Individual nanotube distributions determined from multiple images of the sample shown in Figure 1 for (a) length and (b) height (diameter). Note that the height measurement also includes the dodecyl functional groups. Typically, nanotubes with heights smaller than 2 nm are considered to be individuals. Nanotubes shorter than 30 nm are excluded due to lateral resolution limitations of the AFM tip.

Figure 3. Nanotube rope distributions from multiple images of the sample shown in Figure 1 for (a) length and (b) height (diameter).

Figure 4. Length and diameter distribution of dodecylated single-walled carbon nanotubes. The gray box indicates those nanotubes considered to be individuals. The distribution indicates that 92% of the sample exists as individuals.

Figure 5. Particle distributions from multiple images of the sample shown in Figure 1.

Figure 6. Effect of surface coverage on the measured lengths of individual nanotubes. AFM image showing (a) moderate and (d) high surface coverage. (b and e) Initial length measurements determined from image analysis. (c and f) Length measurements determined from image analysis after manual adjustments by the user. Notice the difference in distribution before and after manual adjustments. For moderate surface coverage, there is little difference suggesting that manual adjustments are unnecessary. Note: the AFM images are not from the same sample.

References

1. E. W. Wong, P. E. Sheehan and C. M. Lieber, Science, 277, 1971 (1997).

2. S. J. Tans, M. H. Devoret, H. J. Dai, A. Thess, R. E. Smalley, L. J. Geerligs and C. Dekker, Nature, 386, 474 (1997).

3. R. V. Seidel, A. P. Graham, J. Kretz, B. Rajasekharan, G. S. Duesberg, M. Liebau, E. Unger, F. Kruepl and W. Hoenlein, Nano Lett., 5, 147 (2005).

4. J. Liu, A. G. Rinzler, H. J. Dai, J. H. Hafner, R. K. Bradley, P. J. Boul, A. Lu, T. Iverson, K. Shelimov, C. B. Huffman, F. Rodriguez-Macias, Y. S. Shon, T. R. Lee, D. T. Colbert and R. E. Smalley, Science, 280, 1253 (1998).

5. Z. Gu, H. Peng, R. H. Hauge, R. E. Smalley and J. L. Margrave, Nano Lett., 2, 1009 (2002).

6. S. R. Lustig, E. D. Boyes, R. H. French, T. D. Gierke, M. A. Harmer, P. B. Hietpas, A. Jagota, R. S. McLean, G. P. Mitchell, G. B. Onoa and K. D. Sams, Nano Lett., 3, 1007 (2003).

7. K. J. Ziegler, Z. Gu, H. Peng, E. L. Flor, R. H. Hauge and R. E. Smalley, J. Am. Chem. Soc., 127, 1541 (2005).

8. V. A. Davis, L. M. Ericson, A. N. G. Parra-Vasquez, H. Fan, Y. Wang, V. Prieto, J. A. Longoria, S. Ramesh, R. K. Saini, C. Kittrell, W. E. Billups, W. W. Adams, R. H. Hauge, R. E. Smalley and M. Pasquali, Macromolecules, 37, 154 (2004).

9. W. Zhou, M. F. Islam, H. Wang, D. L. Ho, A. G. Yodh, K. I. Winey and J. E. Fischer, Chem. Phys. Lett., 384, 185 (2004).

10. N. Sano, M. Naito, M. Chhowalla, T. Kikuchi, S. Matsuda, K. Iimura, H. L. Wang, T. Kanki and G. A. J. Amaratunga, Chemical Physics Letters, 378, 29 (2003).

11. M. F. Islam, E. Rojas, D. M. Bergey, A. T. Johnson and A. G. Yodh, Nano Lett., 3, 269 (2003).

12. J. L. Bahr and J. M. Tour, J. Mater. Chem., 12, 1952 (2002).

13. A. Hirsch, Angew. Chem. Int. Ed., 41, 1853 (2002).

14. M. O'Connell, S. M. Bachilo, C. Huffman, V. C. Moore, M. S. Strano, E. Haroz, K. L. Rialon, P. Boul, W. H. Noon, C. Kittrell, J. Ma, R. H. Hauge, R. B. Weisman and R. Smalley, Science, 297, 593 (2002).

15. V. C. Moore, M. S. Strano, E. H. Haroz, R. H. Hauge and R. E. Smalley, Nano Letters, 3, 1379 (2003).

16. F. Liang, A. K. Sadana, A. Peera, J. Chattopadhyay, Z. Gu, R. H. Hauge and W. E. Billups, Nano Lett., 4, 1257 (2004).

17. Z. Gu, F. Liang, Z. Chen, C. Kittrell, W. E. Billups, R. H. Hauge and R. E. Smalley, Submitted, (2005).

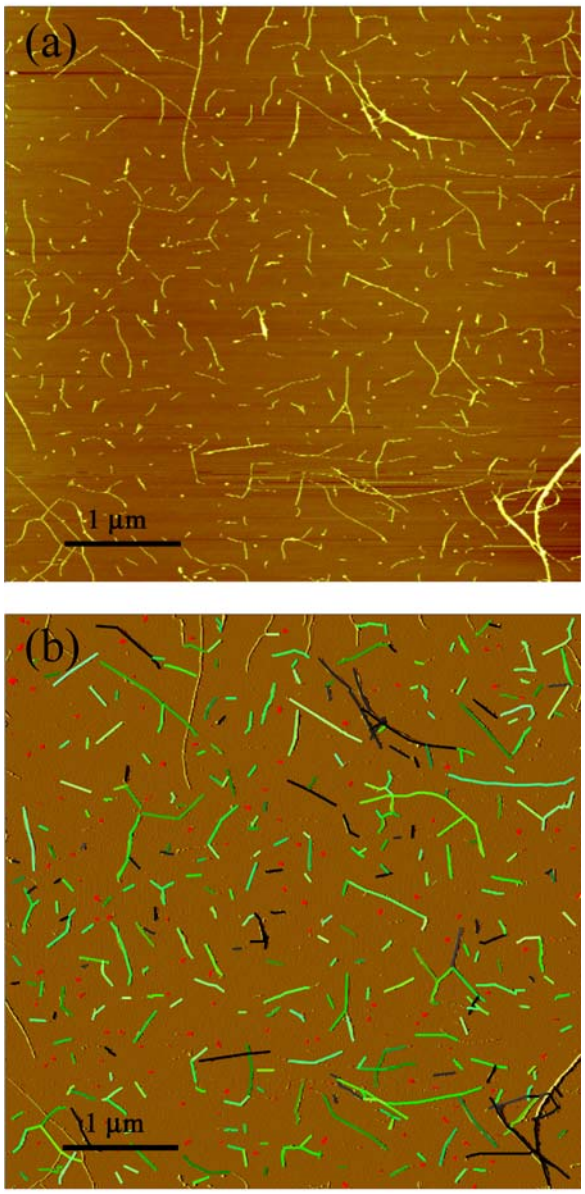
(a)
1 µm
(b)
1 µm

(a)

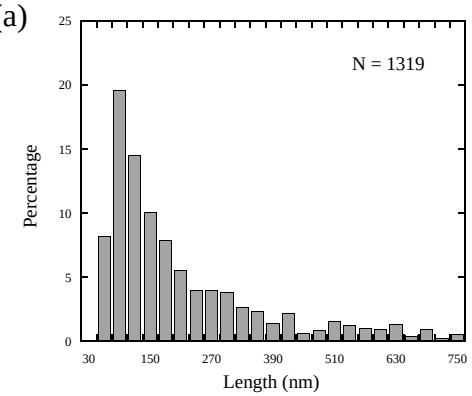
N = 1319
Percentage
Length (nm)
0
5
10
15
20
25
30
150
270
390
510
630
750

(b)

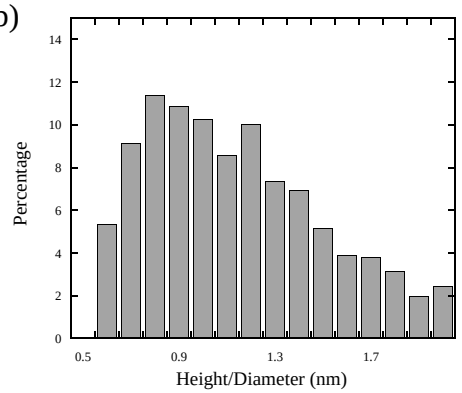
Percentage
Height/Diameter (nm)
0
2
4
6
8
10
12
14
0.5
0.9
1.3
1.7

(a)

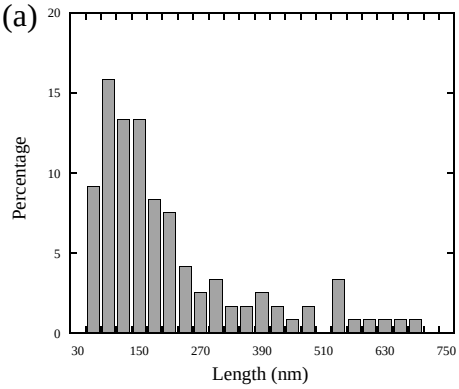
Percentage
0
5
10
15
20
30
150
270
390
510
630
750
Length (nm)

(b)

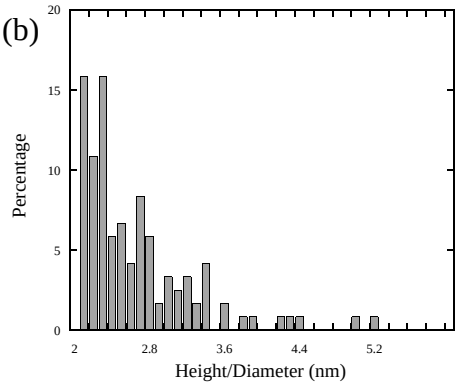
Percentage
0
5
10
15
20
2
2.8
3.6
4.4
5.2
Height/Diameter (nm)

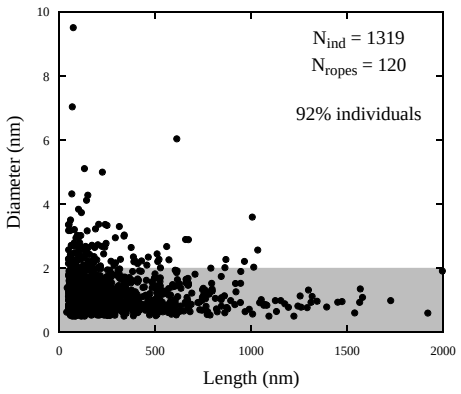
N_{ind} = 1319
N_{ropes} = 120
92% individuals
Diameter (nm)
Length (nm)
0
2
4
6
8
10
0
500
1000
1500
2000

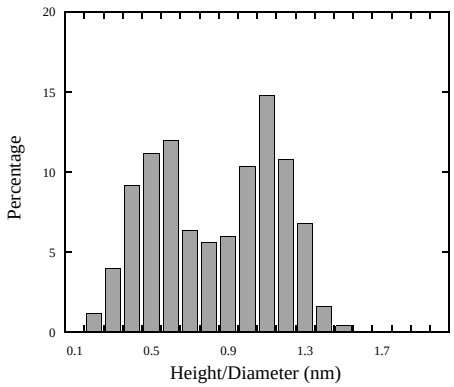
Percentage
20
15
10
5
0
0.1
0.5
0.9
1.3
1.7
Height/Diameter (nm)

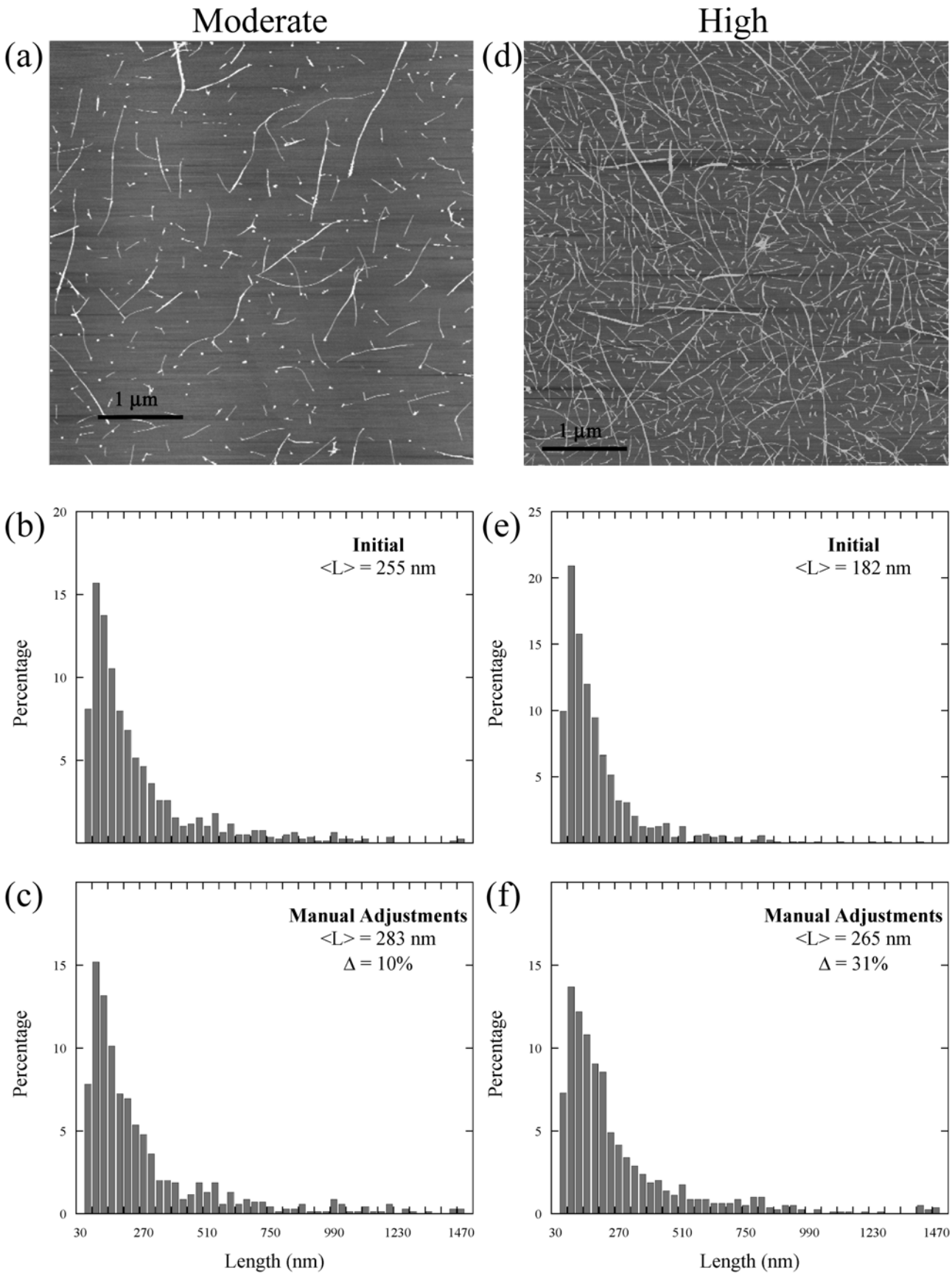
Moderate
High
(a)
(d)
1 µm
1 µm
(b)
(e)
Initial
<L> = 255 nm
Initial
<L> = 182 nm
Percentage
(c)
(f)
Manual Adjustments
<L> = 283 nm
Δ = 10%
Manual Adjustments
<L> = 265 nm
Δ = 31%
Length (nm)
30
270
510
750
990
1230
1470